Electronic Supplementary Information

A Novel Wide-Bandgap Small Molecule Donor for High Efficiency All-Small-Molecule Organic Solar Cells with Small Non-Radiative Energy Losses

Yulong Wang,[†a] Yang Wang, [†a] Lei Zhu,[c] Haiqin Liu,[b] Jin Fang,[a] Xia Guo,[a] Feng Liu,[c] Zheng Tang,[b] Maojie Zhang,*[a] and Yongfang Li[ad]

[a] Laboratory of Advanced Optoelectronic Materials, College of Chemistry, Chemical Engineering and Materials Science, Soochow University, Suzhou 215123, China
E-mail: mjzhang@suda.edu.cn
[b] Center for Advanced Low-dimension Materials, State Key Laboratory for Modification of Chemical Fibers and Polymer Materials, College of Materials Science and Engineering, Donghua University, Shanghai 201620, China
[c] China Frontiers Science Center for Transformative Molecules, School of Chemistry and Chemical Engineering, Shanghai Jiao Tong University, Shanghai 200240, China
[d] Beijing National Laboratory for Molecular Sciences, CAS Key Laboratory of Organic Solids, Institute of Chemistry, Chinese Academy of Sciences, Beijing 100190, China

Experimental Section

Instruments and Measurements

^{1}H NMR and ^{13}C NMR spectra were measured in $CDCl_3$ on Bruker AV 400 MHz FT-NMR spectrometer. UV-vis absorption spectra were taken on an Agilent Technologies Cary Series UV-Vis-NIR Spectrophotometer. Thermogravimetric analysis (TGA) was performed on a Perkin-Elmer TGA-7. Differential scanning calorimetry (DSC) was performed on a TA DSC Q-200. The electrochemical cyclic voltammetry (CV) was performed on a Zahner Ennium IM6 Electrochemical Workstation with glassy carbon disk, Pt wire, and Ag/Ag^+ electrode as working electrode, counter electrode, and reference electrode respectively, in a 0.1 M tetrabutylammonium hexafluorophosphate (Bu_4NPF_6) acetonitrile solution. Photoluminescence (PL) spectra were performed on an Edinburgh Instrument FLS 980.

The current density-voltage (*J-V*) characteristics of the non-fullerene SM-OSCs were recorded with a keithley 2450. The power conversion efficiencies of the SM-OSCs were measured under 1 sun, AM 1.5G (air mass 1.5 global) (100 mW cm^{-2}) using a SS-F5-3A (Enli Technology CO., Ltd.) solar simulator (AAA grade, 50 mm x 50 mm photo-beam size). 2×2 cm^2 Monocrystalline silicon reference cell (SRC-00019, covered with a KG5 filter windows) was purchased from Enli Technology CO., Ltd. The EQE was measured by Solar Cell Spectral Response Measurement System QE-R3011 (Enli Technology CO., Ltd.). The light intensity at each wavelength was calibrated with a standard single-crystal Si photovoltaic cell. Atomic force microscopy (AFM) measurements were performed on a Dimension 3100 (Veeco) Atomic Force Microscope in the tapping mode. Transmission electron microscopy (TEM) was performed using a Tecnai G2 F20 S-TWIN instrument at 200 kV accelerating voltage, in which the blend films were prepared as following: first, the blend films were spin-coated on the PEDOT:PSS/ITO substrates; second, the resulting blend film/PEDOT:PSS/ITO substrates were submerged in deionized water to make these blend films float onto the air-water interface; finally, the floated blend films were

taken up on unsupported 200 mesh copper grids for a TEM measurement. GIXD experiment was performed at beamLine 7.3.3 at the Advanced Light Source,[1] Lawrence Berkeley National Laboratory, Berkeley, CA. Samples were prepared using identical blend solutions as those used in devices on a PEDOT:PSS pre-coated Si substrates.

Device fabrication and characterization

The non-fullerene SM-OSCs devices with a device structure of glass ITO/ poly(3,4-ethylenedioxythiophene):poly(styrenesulfonate) PEDOT:PSS/BTTzR:Y6/PFN-Br/Ag were fabricated under conditions as follows: patterned indium tin oxide (ITO)-coated glass with a sheet resistance of 10-15 ohm/square was cleaned by a surfactant scrub and then underwent a wet-cleaning process inside an ultrasonic bath, beginning with deionized water followed by acetone and isopropanol. After UVO cleaning for 20 min, then a 30 nm thick PEDOT:PSS (Bayer Baytron 4083) anode buffer layer was spin-cast onto the ITO substrate and then annealed at 150 °C for 15 min. The active layer was then deposited on top of the PEDOT:PSS layer by spin-coating a chloroform solution (24 mg mL^{-1}, dissolved 2 h under 60 °C) of BTTzR:Y6. Then the PFN-Br as cathode interlayer was spin-coated on the active layer at 2500 rpm for 40 s. Finally, 150 nm Ag were successively deposited on the photosensitive layer under vacuum at a pressure of ca. 4×10^{-4} Pa. The effective area of one cell is 0.04 cm^2.

Mobility measurement

The mobility was measured by the space charge limited current (SCLC) method by a hole-only device with a structure of ITO/PEDOT:PSS/active layer/MoO_3/Ag or an electron-only device with a structure of ITO/ZnO-gel/active layer/ZnO-NPs/Ag and estimated through the Mott-Gurney equation. For the hole-only devices, SCLC is described by $J \cong (9/8)\varepsilon\varepsilon_0\mu_0 V^2 \exp(0.89\sqrt{V/E_0 L})/L^3$, where ε is the dielectric constant of the polymer, ε_0 is the permittivity of the vacuum, μ_0 is the zero-field mobility, E_0 is the characteristic field, J is the current density, L is the thickness of the blended film, $V = V_{appl} - V_{bi}$, V_{appl} is the applied potential, and V_{bi} is the built-in potential which results from the difference in the work function of the anode and the cathode. For the electron-only devices, SCLC is described by $J = (9/8)\varepsilon_r \varepsilon_0 / \mu_g V^2/L^3$, where J is the current density, ε is the dielectric constant of the polymer, ε_0 is the permittivity of the vacuum, L is the thickness of the blend film, $V = V_{appl} - V_{bi}$, V_{appl} is the applied potential, and V_{bi} is the built-in potential which results from the difference in the work function of the anode and the cathode.

Materials and synthesis

Materials: All chemicals and solvents were reagent grades and purchased from Alfa Aesar and TCI. Compound **1**, Compound **4** were purchased from commercial sources. Compound **2**, compound **3**, compound **5** and **BTTzR** (scheme 1) were synthesized as follows:

Synthesis of compound 2

In a 100 mL flask, compound **1** (2.03 g, 3.82 mmol) was dissolved in a mixture of $CHCl_3$ (25 mL) and acetic acid (25 mL). Under an argon atmosphere and dark against light, NBS (0.71 g, 4.01 mmol) was added to the solution slowly in small portions, and the reaction mixture was stirred for 0.5 h at 0 °C, and then the reaction mixture was stirred for 10 h at room

temperature. The reaction mixture was poured into water (60 mL) and extracted with $CHCl_3$, the organic layer was washed with water for three times and then dried over anhydrous $MgSO_4$. After removal of solvent, the crude product was purified by column chromatography on silica gel using pure petroleum as eluent to afford compound **2** as a yellow solid (1.16 g, 50%), ^{1}H NMR (400 MHz, $CDCl_3$), δ (ppm): 7.38 (s, 1H), 7.21 (s, 1H), 7.04 (d, 1H), 2.56-2.55 (d, 2H), 2.52-2.50 (d, 2H), 1.35-1.29 (m, 18H), 0.93-0.88 (m, 12H): ^{13}C NMR (100 MHz, $CDCl_3$), δ (ppm): 163.08, 161.44, 149.68, 149.66, 143.38, 142.67, 136.85, 136.69, 128.60, 127.59, 124.52, 113.78, 77.22, 77.01, 76.80, 40.30, 39.96, 34.51, 33.88, 32.43, 29.70, 28.85, 28.75, 25.67, 25.59, 23.03, 14.13, 14.12, 10.82. Matrix-Assisted Laser Desorption/Ionization Time of Flight Spectrometry (MALDI-TOF) MS: calcd. for $C_{28}H_{37}BrN_2S_4$ m/z = 609.77; found 611.23.

Synthesis of compound 3

The solution of compound **2** (1.08 g, 1.77 mmol) in $CHCl_3$ (30 mL) was added to a vilsmeier reagent, which was prepared with $POCl_3$ (1.32 mL, 14.16 mmol) in DMF (1.36 mL, 17.7 mmol) at 0 °C, and then the reaction mixture was stirred for 12 h at 65 °C, the mixture was extracted with CH_2Cl_2 (120 mL). The organic layer was washed with water for three times and then dried over anhydrous $MgSO_4$. After removal of solvent, the crude product was purified by column chromatography on silica gel with using petroleum/CH_2Cl_2 (1:1) as eluent to obtain compound **3** as an orange solid (0.99 g, 88%), ^{1}H NMR (400 MHz, $CDCl_3$), δ (ppm): 10.04 (s, 1H), 7.40 (s, 1H), 7.24 (s, 1H), 2.90-2.88 (d, 2H), 2.52-2.51 (d, 2H), 1.38-1.25 (m, 18H), 0.93-0.89 (m, 12H). ^{13}C NMR (100 MHz, $CDCl_3$), δ (ppm): 182.02, 163.07, 160.73, 152.38, 151.25, 150.39, 144.28, 142.90, 139.52, 136.40, 129.39, 128.24, 114.69, 77.23, 77.02, 76.81, 39.96, 32.47, 32.43, 28.76, 28.74, 25.71, 25.67, 23.03, 22.97, 14.12, 14.08, 10.82, 10.80. Matrix-Assisted Laser Desorption/Ionization Time of Flight Spectrometry (MALDI-TOF) MS: calcd. for $C_{29}H_{37}BrN_2OS_4$ m/z = 637.78; found 638.23.

Synthesis of compoud 5

In a 100 mL dried flask, compound **3** (0.87 g, 1.36 mmol), compound **4** (0.59 g, 0.55 mmol) and $Pd(PPh_3)_4$ (0.047 g, 0.04 mmol) were dissolved in anhydrous degassed toluene (50 mL). The mixture was slowly heated up to 110 °C and stirred at the temperature for 24 h under an argon atmosphere. The mixture was poured into water and extracted with CH_2Cl_2 (100 mL) for three times. The organic layer was dried over anhydrous $MgSO_4$ and concentrated under vacuum. The crude product was purified by column chromatography on silica gel with using petroleum/CH_2Cl_2 (1:1) as eluent to obtain compound **5** as a red solid (0.75 g, 73%), ^{1}H NMR (400 MHz, CD_2Cl_2), δ (ppm): 9.98 (s, 2H), 7.74 (s, 2H), 7.37-7.36 (d, 4H), 7.32 (s, 2H), 2.83-2.80 (t, 12H), 2.69-2.66 (t, 4H), 1.50-1.28 (m, 70H), 1.00-0.84 (m, 42H). ^{13}C NMR (100 MHz, $CDCl_3$), δ (ppm): 181.98, 163.36, 160.48, 152.37, 151.49, 150.53, 144.33, 141.10, 139.66, 139.39, 139.05, 136.23, 135.27, 134.64, 130.76, 129.80, 129.30, 123.72, 122.97, 77.19, 76.98, 76.77, 41.72, 41.50, 40.15, 32.85, 32.69, 32.44, 32.40, 31.78, 30.87, 29.32, 28.93, 28.73, 28.56, 28.50, 25.84, 25.67, 23.09, 22.94, 22.70, 14.18, 14.13, 14.05, 10.93, 10.76, 10.72. Matrix-Assisted Laser Desorption/Ionization Time of Flight Spectrometry (MALDI-TOF) MS: calcd. For $C_{104}H_{138}N_4O_2S_{12}$ m/z = 1861.01; found 1860.03.

Synthesis of BTTzR

Compound **5** (0.39 g, 0.21 mmol) was dissolved in dry $CHCl_3$ (40 mL), and five drops of piperidine and 3-butylrhodanine (0.40 g, 2.1 mmol) were added in above solution then. The reation mixture was stirred and refluxed at 65 °C for 12 h under argon. After that, the mixture was extracted with $CHCl_3$ three times, the combined organic phase was washed with water and dried over anhydrous $MgSO_4$. After removal of solvent, the crude product was purified by column chromatography on silica gel with using petroleum/$CHCl_3$ (1:1) as eluent to obtain **BTTzR** as a black solid (0.33 g, 71%), ^{1}H NMR (400 MHz, $CDCl_3$), δ (ppm): 7.90 (s, 2H), 7.80 (s, 2H), 7.41 (d, 2H), 7.39 (s, 2H), 7.27 (s, 2H), 4.10-4.13 (m, 4H), 2.83-2.78 (m, 8H), 2.73-2.72 (d, 4H), 2.65-2.62 (t, 4H), 1.49-1.26 (m, 74H), 0.99-0.84 (m, 52H). ^{13}C NMR (100 MHz, $CDCl_3$), δ (ppm): 191.97, 167.64, 162.98, 160.50, 151.18, 150.66, 149.73, 142.09, 141.10, 139.67, 139.17, 139.07, 136.65, 136.29, 135.66, 135.36, 134.71, 130.68, 129.83, 129.31, 123.73, 122.95, 122.58, 121.98, 77.22, 77.01, 76.80, 44.70, 41.76, 41.32, 40.18, 33.96, 33.40, 32.73, 32.50, 32.45, 32.31, 31.82, 30.91, 29.36, 29.10, 28.96, 28.75, 28.60, 28.54, 25.87, 25.83, 25.76, 23.13, 23.07, 23.01, 22.73, 20.10, 14.21, 14.17, 14.09, 13.70, 10.96, 10.91, 10.75. Matrix-Assisted Laser Desorption/Ionization Time of Flight Spectrometry (MALDI-TOF) MS: calcd. For $C_{118}H_{156}N_6O_2S_{16}$ m/z = 2201.79; found 2202.84.

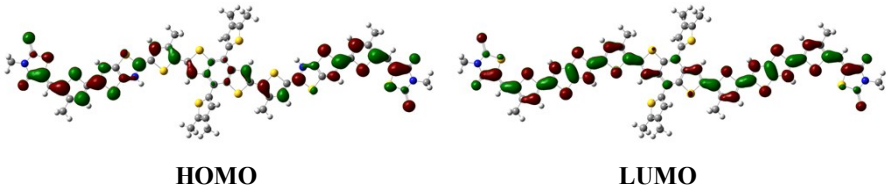

Fig. S1 The frontier molecular orbital of HOMO and LUMO of BTTzR.

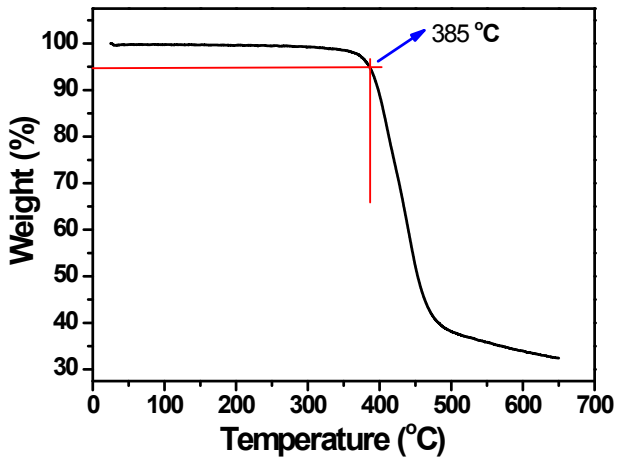

Fig. S2 The TGA curve of BTTzR at a scan rate of 10 °C min^{-1} under nitrogen.

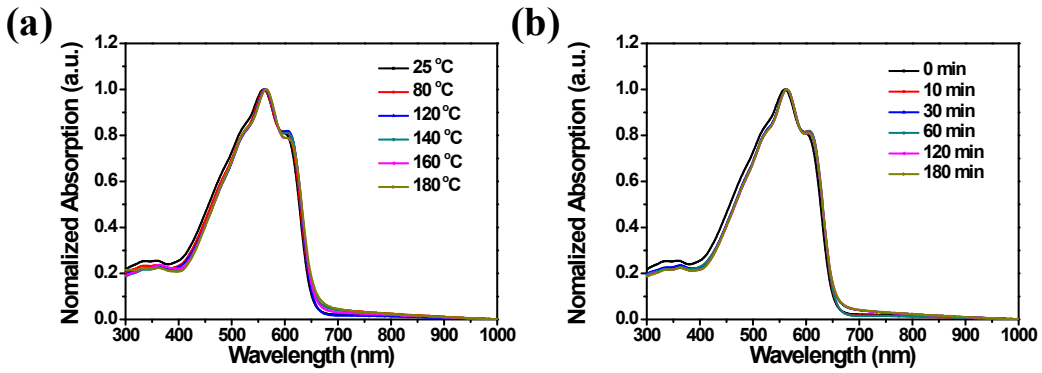

Fig. S3 The absorption of BTTzR film with variety of temperature (a) and variety of time with temperature of 120 °C (b).

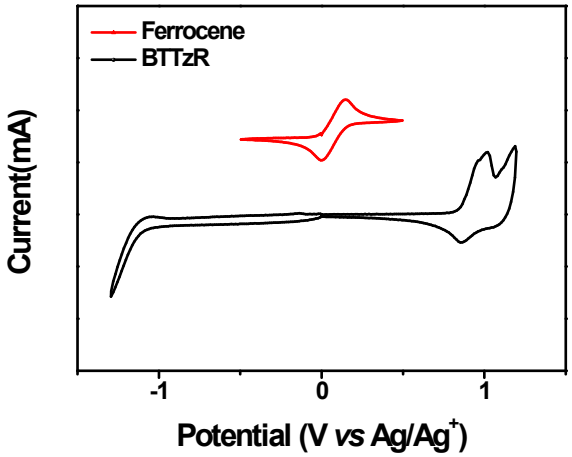

Fig. S4 Cyclic voltammogram of **BTTzR** film on a glassy carbon electrode measured in 0.1 mol L^{-1} Bu_4NPF_6 acetonitrile solution at a scan rate of 50 mV s^{-1}

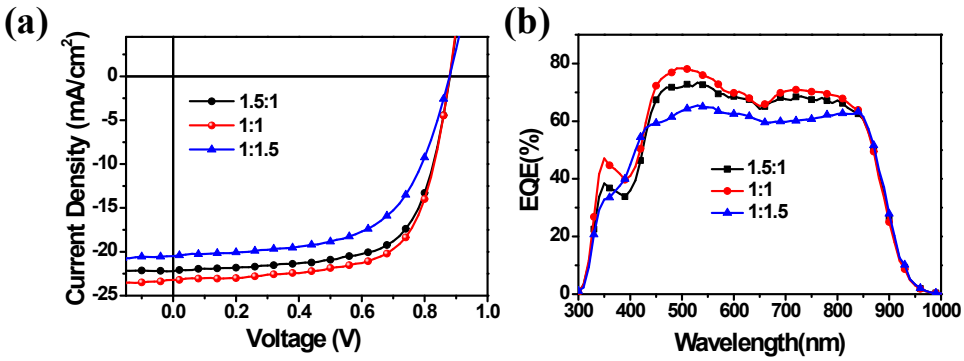

Fig. S5 (a) *J-V* curves and (b) EQE curves of the OSCs based on BTTzR: Y6 blend with different D/A weight ratios under the condition of SVA treatment for 90s.

Table S1. With CS_2-SVA treatment for 90 s, photovoltaic parameters of the OSCs based on **BTTzR**:Y6 blend with different D/A weight ratios under the illumination of AM 1.5G, 100 mW cm^{-2}.

D/A (w/w)	V_{oc} (V)	J_{sc} (mA cm^{-2})	*Cal.* J_{sc}[a] (mA cm^{-2})	FF	PCE (%)
1.5:1	0.88 (0.88±0.01)	22.2 (22.0±0.2)	21.8	0.67 (0.66±0.01)	13.1 (12.9±0.2)
1:1	0.88 (0.88±0.01)	23.2 (23.0±0.2)	22.6	0.68 (0.67±0.01)	13.9 (13.7±0.2)
1:1.5	0.88 (0.88±0.01)	20.5 (20.2±0.3)	20.2	0.60 (0.59±0.01)	10.8 (10.6±0.2)

[a] values calculated from EQE. The average values and standard deviations of the device parameters based on 8 devices are shown in brackets.

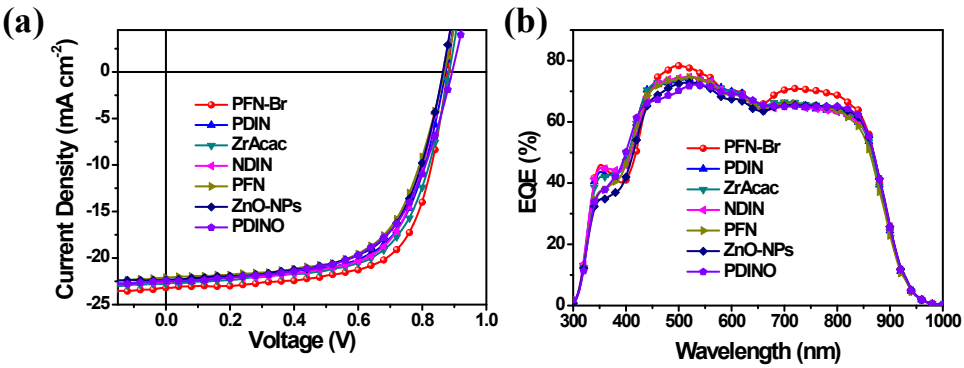

Fig. S6 (a) *J*–*V* curves and (b) EQE curves of the OSCs based on **BTTzR**:Y6 blend with different cathode interfacial layer under the condition of SVA treatment for 90s.

Table S2. Photovoltaic parameters of the OSCs based on **BTTzR**:Y6 (1:1, w/w) blend with different cathode interfacial layer under the illumination of AM 1.5G, 100 mW cm^{-2}.

Interface layer	V_{oc} (V)	J_{sc} (mA cm^{-2})	*Cal.* J_{sc}[a] (mA cm^{-2})	FF	PCE (%)
PFN-Br	0.88 (0.87±0.01)	23.2 (23.0±0.02)	22.6	0.68 (0.67±0.01)	13.9 (13.7±0.2)
PDIN	0.87 (0.86±0.01)	22.6 (22.4±0.02)	21.9	0.64 (0.63±0.01)	12.6 (12.4±0.2)
ZrAcac	0.88 (0.87±0.01)	23.0 (22.8±0.02)	22.0	0.64 (0.63±0.01)	13.0 (12.8±0.2)
NDIN	0.87 (0.86±0.01)	22.5 (22.3±0.02)	21.8	0.66 (0.65±0.01)	12.9 (12.7±0.2)
PFN	0.87 (0.86±0.01)	22.2 (22.0±0.02)	21.6	0.62 (0.61±0.01)	12.0 (11.8±0.2)
ZnO-NPs	0.87 (0.86±0.01)	22.4 (22.2±0.02)	21.5	0.63 (0.62±0.01)	12.3 (12.1±0.2)
PDINO	0.89 (0.88±0.01)	22.4 (22.2±0.02)	21.7	0.61 (0.60±0.01)	12.2 (12.0±0.2)

[a] values calculated from EQE. The average values and standard deviations of the device parameters based on 8 devices are shown in brackets.

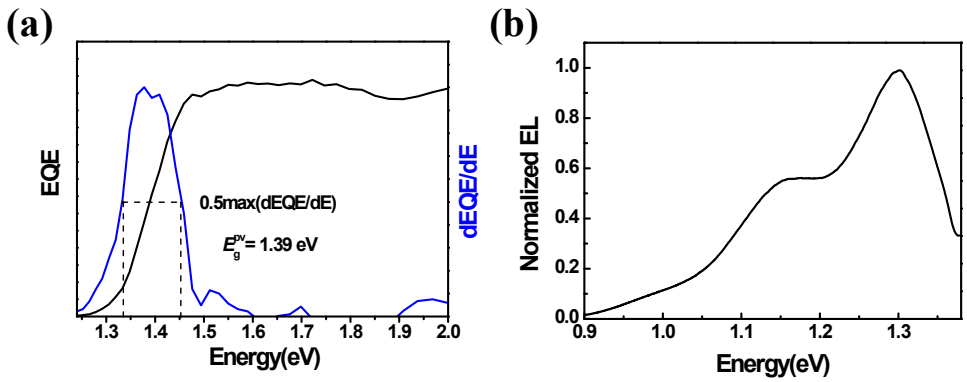

Fig. S7 (a) Deduction of photovoltaic bandgap from the definition of *E*PV g. (b) Electroluminescence (EL) curve of pure acceptor Y6-based device.

Table S3. Comparison between Inorganic and some representative Organic solar cells.

Type of solar cell	Materials	E_g (eV)	V_{oc} (V)	E_{loss} (eV)	ΔE_{nr} (eV)	Ref.
Inorganics	c-Si	1.12	0.68	0.44	0.18	[2]
	Perovskite (evaporated)	1.61	1.08	0.53	0.25	[2]
Organics	**BTTzR:Y6**	**1.39**	**0.88**	**0.51**	**0.18**	**This work**
	P3HT:$PC_{71}BM$	1.93	0.58	1.35	0.38	[2]
	PTB7:$PC_{71}BM$	1.61	0.74	0.87	0.39	[2]
	P3TEA:SF-PDI_2	1.72	1.11	0.61	0.26	[3]
	PBDB-T:Y1	1.44	0.87	0.57	0.25	[4]
	PTB7-Th:IEICO	1.45	0.90	0.55	0.23	[5]
	PBDT-TS1:T-2	1.62	1.01	0.61	0.27	[6]
	PBDB-TF:IO-4Cl	1.80	1.24	0.56	0.25	[7]
	ZnPc:C60	1.53	0.56	0.97	0.38	[8]
	PBDB-T:IDTT2F	1.46	0.81	0.65	0.27	[9]
	PM6:Y6	1.39	0.83	0.56	0.25	[10]
	ZR1:Y6	1.38	0.86	0.52	0.24	[11]
	PBDB-T:DOC6-IC	1.43	0.91	0.52	0.20	[12]
	PBDB-T:DOC2C6-2F	1.42	0.85	0.57	0.27	[12]

Table S4. Photovoltaic results of recent high performance SM-OSCs devices.

Type	Materials	E_g (eV)	E_{loss} (eV)	V_{oc} (V)	PCE_{max} (%)	Ref.
Fullerene SM-OSCs	BTID-1F:$PC_{71}BM$	1.55	0.81	0.94	10.40	[13]
	DR3TSBDT:$PC_{71}BM$	1.73	0.82	0.91	9.95	[14]
	BDTTNTTR:$PC_{71}BM$	1.51	0.62	0.89	10.02	[15]
	BDTSTNTTR:$PC_{71}BM$	1.56	0.63	0.93	11.53	[15]
	O-BDTdFBT:$PC_{71}BM$	1.83	0.97	0.86	8.10	[16]
	BTR:$PC_{71}BM$	1.82	0.90	0.92	9.30	[17]
	DRCN5T:$PC_{71}BM$	1.60	0.92	0.68	10.08	[18]
Non-fullerene SM-OSCs	**BTTzR:Y6**	**1.39**	**0.51**	**0.88**	**13.90**	**This work**
	DRTB-T:IC-C6IDT-IC	1.62	0.64	0.98	9.08	[19]
	DRTB-T:IDIC	1.62	0.64	0.98	9.06	[20]
	DRTB-T-C4:IT-4F	1.54	0.63	0.91	11.24	[21]
	H22:IDIC	1.63	0.68	0.94	10.29	[22]
	SM1:IDIC	1.63	0.72	0.91	10.11	[23]
	H11:IDIC	1.63	0.65	0.98	9.73	[24]
	NDTSR:IDIC	1.63	0.71	0.92	8.05	[25]
	BDT3TR-SF:NBDTP-Fout	1.41	0.61	0.80	11.25	[26]
	ZnP-TBO:6TIC	1.37	0.57	0.80	12.08	[27]
	BSFTR:NBDTP-F_{out}	1.41	0.61	0.80	12.26	[28]
	BTR-Cl:Y6	1.33	0.47	0.86	13.61	[29]
	BSFTR:Y6	1.33	0.48	0.85	13.69	[30]
	ZR1:Y6	1.38	0.52	0.86	14.34	[11]

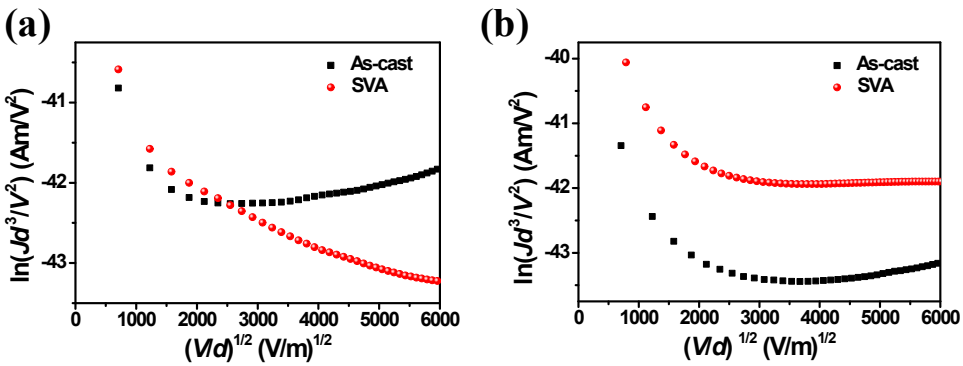

Fig. S8 ln(Jd^3/V^2) *vs* $(V/d)^{1/2}$ plots of (a) the hole-only devices with the structure of ITO/PEDOT:PSS/active layer/MoO_3/Ag, and (b) the electron-only devices with the structure of ITO/ZnO-gel/active layer/ZnO-NPs/Ag.

Table S5. Mobilities of pure films, **BTTzR**:Y6 (1:1, w/w) blend films of As-cast and with SVA treatment.

	μ_h ($cm^2\ V^{-1}\ s^{-1}$)	μ_e ($cm^2\ V^{-1}\ s^{-1}$)	μ_e/μ_h
BTTzR	3.39×10^{-4}	-	-
Y6	-	9.92×10^{-4}	-
As-cast	7.51×10^{-5}	3.15×10^{-5}	0.42
SVA[a)]	1.79×10^{-4}	1.82×10^{-4}	1.02

[a)] SVA treatment for 90 s.

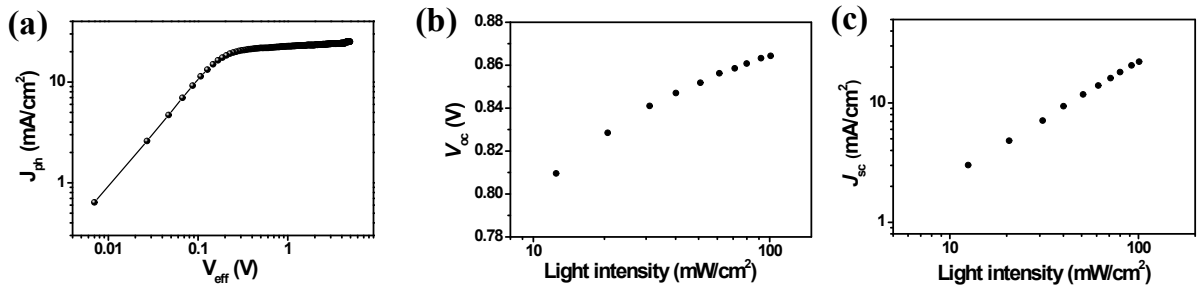

Fig. S9 (a) J_{ph} versus V_{eff} characteristics. the dependence of V_{oc} (b) and J_{ph} (c) on light intensity for the SM-OSCs based on BTTzR:Y6 (1:1, w/w) with SVA treatment for 90 s.

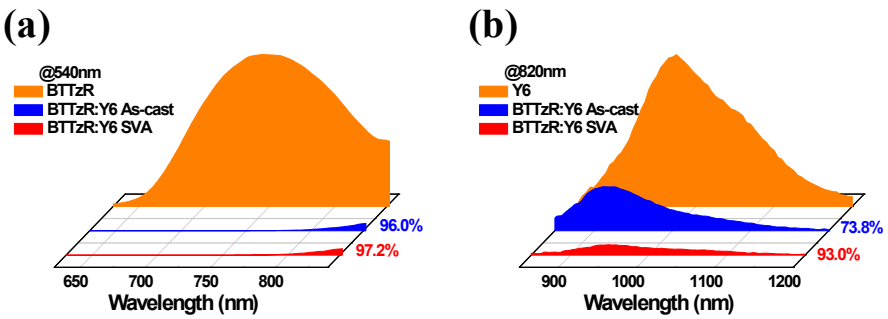

Fig. S10 (a) and (b) The PL spectra of BTTzR, Y6 and the related blend films (excited at 540 nm for BTTzR, and 820 nm for Y6 and the their blend films).

Table S6. *d*-spacing and cohenrence length of **BTTzR**, Y6, As-cast and with SVA treatment.

	IP				OOP			
	100		010		100		010	
	d [a] (Å)	CCL [b] (nm)	d [a] (Å)	CCL [b] (nm)	d [a] (Å)	CCL [b] (nm)	d [a] (Å)	CCL [b] (nm)
BTTzR	17.45	8.30	3.65	0.26	15.71	8.88	3.64	1.39
Y6	22.41	4.81	3.63	0.18	-	-	3.66	2.14
As-cast	19.32	5.49	-	-	-	-	3.53	1.87
SVA	17.55	7.14	3.61	0.19	15.32	2.29	3.50	2.61

[a] d = d-spacing (Å). [b] CCL = crystal coherence length (nm).

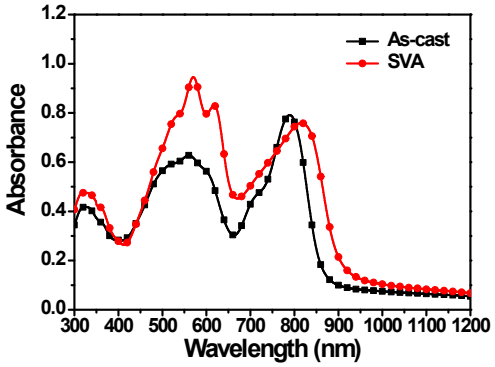

Fig. S11 Absorption spectra of blend films of As-cast and SVA treatment for 90s.

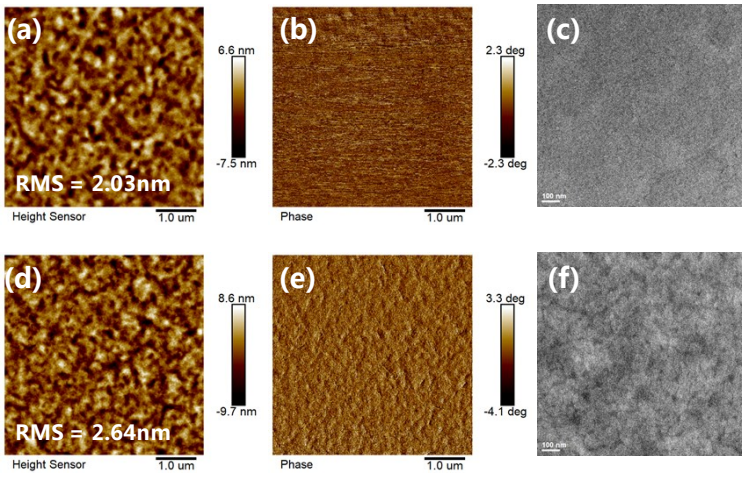

Fig. S12 AFM and TEM images: (a), (b) and (c) for the As-cast blend films; (d), (e) and (f) for the blend films with SVA treatment for 90 s.

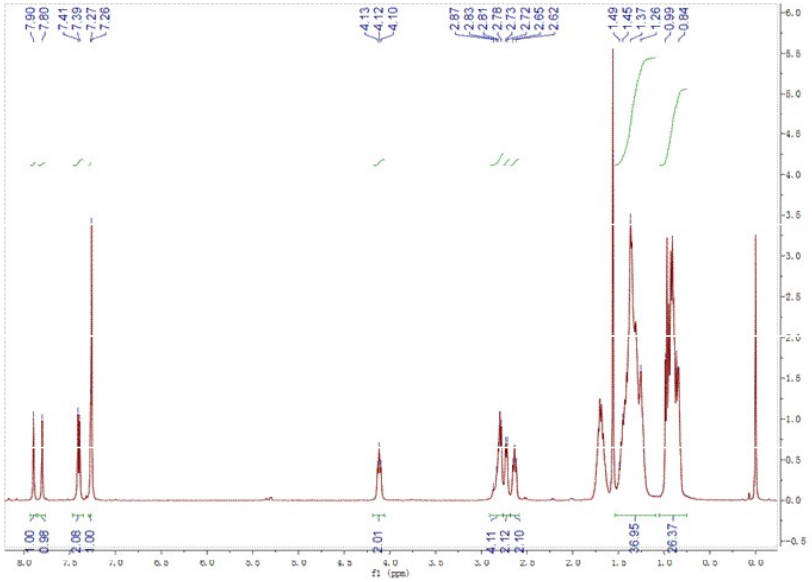

Fig. S13 ^{1}H NMR spectra of BTTzR in $CDCl_3$.

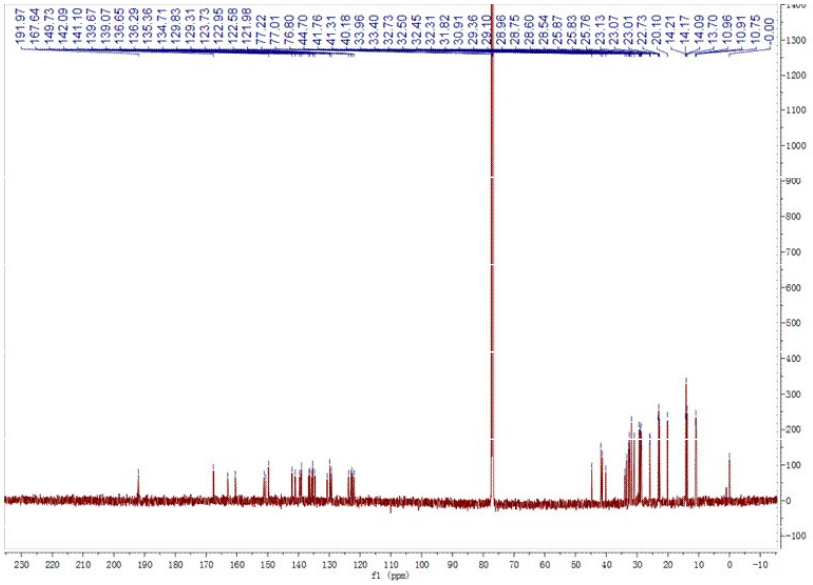

Fig. S14 ^{13}C NMR spectra of BTTzR in $CDCl_3$.

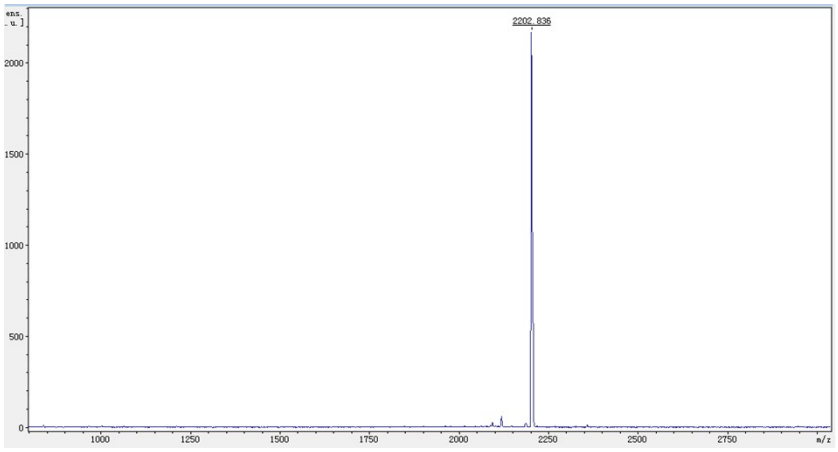

Fig. S15 MALDI-TOF spectra of BTTzR.

References

1 W. Ma, J. R. Tumbleston, M. Wang, E. Gann, F. Huang and H. Ade, *Adv. Energy Mater.,* 2013, **3**, 864-872.

2 J. Yao, T. Kirchartz, M. S. Vezie, M. A. Faist, W. Gong, Z. He, H. Wu, J. Troughton, T. Watson, D. Bryant and J. Nelson, *Phys. Rev. Appl.,* 2015, **4**, 014020.

3 J. Liu, S. Chen, D. Qian, B. Gautam, G. Yang, J. Zhao, J. Bergqvist, F. Zhang, W. Ma, H.

Ade, O. Inganäs, K. Gundogdu, F. Gao and H. Yan, *Nat. Energy,* 2016, **1**, 16089.

4 J. Yuan, T. Huang, P. Cheng, Y. Zou, H. Zhang, J. L. Yang, S. Y. Chang, Z. Zhang, W. Huang, R. Wang, D. Meng, F. Gao and Y. Yang, *Nat. Commu.,* 2019, **10**, 570.

5 D. Qian, Z. Zheng, H. Yao, W. Tress, T. R. Hopper, S. Chen, S. Li, J. Liu, S. Chen, J. Zhang, X. K. Liu, B. Gao, L. Ouyang, Y. Jin, G. Pozina, I. A. Buyanova, W. M. Chen, O. Inganas, V. Coropceanu, J. L. Bredas, H. Yan, J. Hou, F. Zhang, A. A. Bakulin and F. Gao, *Nat. Mater.,* 2018, **17**, 703-709.

6 H. Fu, Y. Wang, D. Meng, Z. Ma, Y. Li, F. Gao, Z. Wang and Y. Sun, *ACS Energy Letters,* 2018, **3**, 2729-2735.

7 Y. Cui, Y. Wang, J. Bergqvist, H. Yao, Y. Xu, B. Gao, C. Yang, S. Zhang, O. Inganäs, F. Gao and J. Hou, *Nat. Energy,* 2019, **4**, 768-775.

8 K. Vandewal, J. Benduhn and V. C. Nikolis, *Sustain. Energy Fuels,* 2018, **2**, 538-544.

9 Y. Liu, M. Li, J. Yang, W. Xue, S. Feng, J. Song, Z. Tang, W. Ma and Z. Bo, *Adv. Energy Mater.,* 2019, **9**, 1901280.

10 R. Yu, H. Yao, Y. Cui, L. Hong, C. He and J. Hou, *Adv. Mater.,* 2019, **31**, 1902302.

11 R. Zhou, Z. Jiang, C. Yang, J. Yu, J. Feng, M. A. Adil, D. Deng, W. Zou, J. Zhang, K. Lu, W. Ma, F. Gao and Z. Wei, *Nat. Commu.,* 2019, **10**, 5393.

12 H. Huang, Q. Guo, S. Feng, C. Zhang, Z. Bi, W. Xue, J. Yang, J. Song, C. Li, X. Xu, Z. Tang, W. Ma and Z. Bo, *Nat. Commu.,* 2019, **10**, 3038.

13 D. Deng, Y. Zhang, J. Zhang, Z. Wang, L. Zhu, J. Fang, B. Xia, Z. Wang, K. Lu, W. Ma and Z. Wei, *Nat. Commun.*, 2016, **7**, 13740.

14 B. Kan, Q. Zhang, M. Li, X. Wan, W. Ni, G. Long, Y. Wang, X. Yang, H. Feng and Y. Chen, *J. Am. Chem. Soc.*, 2014, **136**, 15529-15532.

15 J. Wan, X. Xu, G. Zhang, Y. Li, K. Feng and Q. Peng, *Energy Environ. Sci.*, 2017, **10**, 1739-1745.

16 L. Yuan, Y. Zhao, J. Zhang, Y. Zhang, L. Zhu, K. Lu, W. Yan and Z. Wei, *Adv. Mater.*,

2015, **27**, 4229-4233.

17 K. Sun, Z. Xiao, S. Lu, W. Zajaczkowski, W. Pisula, E. Hanssen, J. M. White, R. M. Williamson, J. Subbiah, J. Ouyang, A. B. Holmes, W. W. Wong and D. J. Jones, *Nat. Commun.*, 2015, **6**, 6013.

18 B. Kan, M. Li, Q. Zhang, F. Liu, X. Wan, Y. Wang, W. Ni, G. Long, X. Yang, H. Feng, Y. Zuo, M. Zhang, F. Huang, Y. Cao, T. P. Russell and Y. Chen, *J. Am. Chem. Soc.*, 2015, **137**, 3886-3893.

19 L. Yang, S. Zhang, C. He, J. Zhang, H. Yao, Y. Yang, Y. Zhang, W. Zhao and J. Hou, *J. Am. Chem. Soc.*, 2017, **139**, 1958-1966.

20 S. Zhang, L. Yang, D. Liu, C. He, J. Zhang, Y. Zhang and J. Hou, *Sci. Chin. Chem.*, 2017, **60**, 1340-1348.

21 L. Yang, S. Zhang, C. He, J. Zhang, Y. Yang, J. Zhu, Y. Cui, W. Zhao, H. Zhang, Y. Zhang, Z. Wei and J. Hou, *Chem. Mater.*, 2018, **30**, 2129-2134.

22 H. Bin, J. Yao, Y. Yang, I. Angunawela, C. Sun, L. Gao, L. Ye, B. Qiu, L. Xue, C. Zhu, C. Yang, Z.-G. Zhang, H. Ade and Y. Li, *Adv. Mater.*, 2018, **30**, 1706361.

23 B. Qiu, L. Xue, Y. Yang, H. Bin, Y. Zhang, C. Zhang, M. Xiao, K. Park, W. Morrison, Z.-G. Zhang and Y. Li, *Chem. Mater.*, 2017, **29**, 7543-7553.

24 H. Bin, Y. Yang, Z. Zhang, L. Ye, M. Ghasemi, S. Chen, Y. Zhang, C. Zhang, C. Sun, L. Xue, C. Yang, H. Ade and Y. Li, *J. Am. Chem. Soc.*, 2017, **139**, 5085-5094.

25 H. Li, Y. Zhao, J. Fang, X. Zhu, B. Xia, K. Lu, Z. Wang, J. Zhang, X. Guo and Z. Wei, *Adv. Energy Mater.*, 2018, **8**, 1702377.

26 H. Wu, H. Fan, S. Xu, L. Ye, Y. Guo, Y. Yi, H. Ade and X. Zhu, *Small*, 2019, **15**, 1804271.

27 K. Gao, S. B. Jo, X. Shi, L. Nian, M. Zhang, Y. Kan, F. Lin, B. Kan, B. Xu, Q. Rong, L. Shui, F. Liu, X. Peng, G. Zhou, Y. Cao and A. K. Jen, *Adv. Mater.*, 2019, **31**, 1807842.

28 H. Wu, Q. Yue, Z. Zhou, S. Chen, D. Zhang, S. Xu, H. Zhou, C. Yang, H. Fan and X.

Zhu, *J. Mater. Chem. A*, 2019, **7**, 15944-15950.

29 H. Chen, D. Hu, Q. Yang, J. Gao, J. Fu, K. Yang, H. He, S. Chen, Z. Kan, T. Duan, C. Yang, J. Ouyang, Z. Xiao, K. Sun and S. Lu, *Joule*, 2019, **3**, 3034-3047.

30 Q. Yue, H. Wu, Z. Zhou, M. Zhang, F. Liu and X. Zhu, *Adv. Mater.*, 2019, **31**, 1904283.